Spectrochimica Acta Part A: Molecular and Biomolecular Spectroscopy 329 (2025) 125518

Contents lists available at ScienceDirect

Spectrochimica Acta Part A:
Molecular and Biomolecular Spectroscopy

journal homepage: www.journals.elsevier.com/spectrochimica-acta-part-a-molecular-and-biomolecular-spectroscopy

Review Article

Accuracy of Raman spectroscopy in discriminating normal brain tissue from brain tumor: A systematic review and *meta*-analysis

Anastasija Krzemińska [b,*], Bogdan Czapiga [a,b], Marta Koźba-Gosztyła [b]

[a] *Faculty of Medicine, Wroclaw University of Science and Technology, Grunwaldzki square 11, 51-377 Wrocław, Poland*
[b] *Department of Neurosurgery, 4th Military Hospital in Wroclaw, Wrocław, Poland*

HIGHLIGHTS

- Raman spectroscopy has a potential to serve as a tool for differentiation of brain tumor from normal brain tissue.
- Raman spectroscopy could be helpful in distinguishing malignant lesion from benign with high sensitivity and specificity.
- Raman spectroscopy could be helpful in identification of tumor type with high sensitivity and specificity.
- There is a need for more studies on Raman spectroscopy accuracy in differentiation of brain tumor types and subtypes, especially in vivo.

GRAPHICAL ABSTRACT

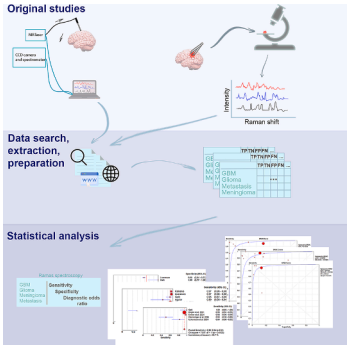

ARTICLE INFO

Keywords:
Raman spectroscopy
Brain tumor
Brain surgery
Tumor borders
Intraoperative

ABSTRACT

Importance: There are several methods of intraoperative tumor border identification, but none of them is perfect. There is a need of a new tool.

Objective: Raman spectroscopy, being a noninvasive, requiring no tissue preparation, quick technique of substance structure identification, is a potential tool for intraoperative identification of brain tumor. This *meta*-analysis aimed to assess the accuracy of Raman spectroscopy in differentiation of normal brain tissue from brain tumor.

Data sources: PubMed, Google Scholar, Scopus and Web of Science databases were searched until October 1, 2024.

Study selection: All English-language articles reporting efficacy and accuracy of Raman spectroscopy for brain tumor differentiation were analyzed, sufficient data to construct 2x2 table was extracted. Exclusion criteria: studies using data from national databases; reviews, conference abstracts, case studies, letters to the editor; studies with irrelevant or not sufficient data; not human tissue used in the experiment. 6112 records were found; after exclusion, the suitability of 64 full-text articles was evaluated. 18 studies were reviewed and included into the *meta*-analysis.

Data extraction and synthesis: The *meta*-analysis was performed in accordance with PRISMA guidelines and recommendations. Methodological quality was assessed according to the QUADAS-2 guidelines. Data were extracted

* Corresponding author at: Department of Neurosurgery, 4th Military Hospital in Wroclaw, Wrocław, Poland.
E-mail addresses: anastasijakrzeminska@gmail.com, neurochirurgia.lekarze@4wsk.pl (A. Krzemińska).

https://doi.org/10.1016/j.saa.2024.125518
Received 21 June 2024; Received in revised form 24 November 2024; Accepted 27 November 2024
Available online 30 November 2024

by multiple observers and any discrepancies were resolved by discussion and consensus. Data were pooled using a random-effects model.
Main outcome(s) and measure(s): The primary outcome was pooled sensitivity, specificity and diagnostic odds ratio (DOR) for Raman spectroscopy.
Results: The manuscript presents 18 studies which were used to calculate pooled values. The pooled sensitivity, specificity and pooled diagnostic odds ratio (DOR) of RS for discriminating glioma and normal brain tissues were 0,965, 0,738 and 61,305 respectively. For GBM the results were 0,948, 0,506 and 78,420 respectively. For meningioma pooled values were 0,896, 0,913, and 149,59. For metastases pooled values were 0,946, 0,862 and 133,90 respectively.
Conclusions and relevance: Raman spectroscopy has a potential to serve as a tool for differentiation of brain tumor from normal brain tissue. Not only could it be helpful in distinguishing malignant lesion from benign with high sensitivity and specificity, but also indicate type of tumor. There is a need for more studies examining the accuracy of spectroscopy in differentiating brain tumors from healthy tissues, especially in vivo and in differentiation of brain tumor subtypes.

Key points

- **Question:** Is Raman spectroscopy (RS) an effective tool for distinguishing of normal brain tissue from brain tumor?
- **Findings:** The pooled sensitivity, specificity and pooled diagnostic odds ratio (DOR) of RS for discriminating glioma and normal brain tissues were 0,965, 0,738 and 61,305 respectively. For GBM the results were 0,948, 0,506 and 78,420 respectively. For meningioma pooled values were 0,896, 0,913, and 149,59. For metastases pooled values were 0,946, 0,862 and 133,90 respectively.
- **Meaning:** Raman spectroscopy has a potential to serve as a tool for differentiation of brain tumor from normal brain tissue. Not only could it be helpful in distinguishing malignant lesion from benign with high sensitivity and specificity, but also indicate type of tumor.

1. Introduction

Central Nervous System (CNS) tumors are the third most common type of cancer and the third leading cause of cancer-related death among adolescents and young adults (ages 15–39) [1], whereas in children under the age of 20 brain tumors are the leading cause of cancer death globally [5]. Approximately 90,000 people receive a primary brain tumor diagnosis annually [2]. Almost 36 % of primary brain tumors are malignant [3,4,6]. Survival outcome for primary brain tumors mostly depends on patient's age, tumor location within brain and thus surgical treatment possibilities and tumor's grade. CNS World Health Organization (WHO) grade 1 tumors have the best relative survival rate, and CNS WHO grade 4 tumors have the worst survival rate, with only 6,8% of patients living for five years after diagnosis [7].

The most common types of primary brain tumors are gliomas, meningiomas, and pituitary adenomas [3].

If tumor is resectable, glioma surgery aims to extensively remove tumor tissue infiltrating the brain while not causing damage to critical brain structures at the same time. The more extensive the resection of glioma tissue, the better survival outcome is expected [8,9].

One of the limitations for glioma extensive removal, apart from patient's neurological deficits and poor quality of life, is the fact that the tumor border is mostly blurred due to the infiltrative growth of tumor tissue. It is essential for neurosurgeon to be able to differentiate intraoperatively brain tissue infiltrated with tumor from healthy one. Currently there is no such technique that could provide quick, effective, reliable and affordable for most centers differentiation of glioma from normal brain tissue and therefore there is a need to find such a method.

Nowadays there are several methods that can be used to facilitate identification of tumor borders at the operating room: intraoperative neuronavigation, intraoperative fluorescence-guided microsurgery, intraoperative frozen section, intraoperative MRI and intraoperative ultrasound. Unfortunately none of the above fulfills the requirements of perfect visualization tool [10,11].

In recent decades Raman spectroscopy (RS) is reported to be a promising method of cancer diagnosis of different tissues such as brain, skin, breast, colorectal, gastric, esophagus, larynx, cervix and urogenital tract [12,13,14].

RS is a technique of substance identification based on the analysis of light scattering off the surface of the substance after it has been illuminated with a laser.

RS is a non-contact technique that does not require sample preparation, so it can analyze nearly each sample without damaging it [15]. This noninvasiveness along with rapidity of RS method makes it a potential tool for intraoperative identification of tissue type.

RS can be performed either ex vivo (tissue sample is excised and placed onto a spectrometer slide) or in vivo (a custom-built handheld probe performs Raman analysis during direct contact with brain tissue intraoperatively) [37,42].

This *meta*-analysis aimed to give a systematic evaluation of the accuracy of RS for discriminating brain tumor and healthy brain tissues.

2. Methods

2.1. Overview

The *meta*-analysis was performed in accordance with the preferred reporting items for systematic reviews and *meta*-analyses (PRISMA) guidelines and recommendations [30,31]. PRISMA checklist can be found in Appendix 3.

2.2. Search strategy

An electronic search of articles reporting data on accuracy of RS for brain tumor differentiation was performed – PubMed, Google Scholar, Scopus and Web of Science databases were searched until October 1, 2024. All titles and abstracts were reviewed for suitability and afterwards the full texts of potentially relevant articles were retrieved so as to perform a thorough eligibility analysis based on the selection criteria. Any discrepancies during the selection and extraction processes were resolved by discussion and consensus.

2.3. Selection criteria

All English-language articles that reported on efficacy and accuracy or RS for brain tumor differentiation were analyzed, sufficient data to construct 2x2 table was extracted. The criteria for excluding studies were: (1) studies which did not present brain tumor types, analyzed RS accuracy only for tumor vs non-tumor tissue differentiation [63,65,68–70]; (2) studies that used data from national databases; (3) reviews, conference abstracts, case studies, and letters to the editor; (4) studies with irrelevant data [53,54,57,58,61,64,66,71,72]; (5) not human tissue used in the experiment; (6) studies from which true positive (TP), true negative (TN), false positive (FP) and false negative (FN)

values could not have been extracted [48–52,55,56,59,60,62,67]; (7) studies where TP, TN, FP, FN values were given for samples or patient count, but not for spectra [42,74,78].

2.4. Outcomes

The primary outcome of interest was Raman's spectroscopy effectiveness as a method of brain tumor identification.

2.5. Data extraction

Extracted data from included articles was put into a spreadsheet using Microsoft Excel (2019; Microsoft Corporation, Redmond, WA, USA). We recorded: the first author's last name and year of publication as a study identifier; number of total patients; number of patients in test group (not training); number of tissues; number of spectra; tumor type; mean age; sample type; cross validation; diagnostic algorithm; RS type; number of true positive (TP), false positive (FP), true negative (TN) and false negative (FN) or, if TP, FP, TN, FN were not available, 95 % confidence intervals of sensitivity, specificity and accuracy of RS.

Table 1
Detailed characteristics of the 18 studies.

Study	Sample type	N1	N2	N3	N4	Tumor type
Koljenovic et al. 2005 [27]	ex vivo	20	20	38	115	meningioma
Leslie et al. 2012 [33]	ex vivo	44	28	64	649	glioma
Aguiar et al. 2013 [34]	ex vivo	–	–	–	172	GBM, meningioma, medulloblastoma
Kalkanis et al. 2014 [35]	ex vivo	17	17	40	1198	GBM
Jermyn et al. 2015 [37]	in vivo	17	15	–	161	glioma
Ji et al. 2015 [36]	ex vivo	22	19	53	1684	glioma
Galli et al. 2019 [38]	ex vivo	209	202		1070	glioma, GBM, metastases, meningioma
Riva et al. 2021 [29]	ex vivo	63*	38*	63	3450	glioma
Livermore et al. 2021 [40]	ex vivo	73	62	73	11,624	glioma, GBM
Jabarkheel et al. 2022 [41]	ex vivo	29	20	160	678	glioma
Kopec et al. 2021 [73]	ex vivo	8	8	–	135,600	metastasis, GBM, glioma, meningioma, pituitary adenoma, neurofibroma
Auner et al. 2012 [75]	ex vivo	–	–	19	435	glioma, medulloblastoma
Klamminger et al. 2021 [76]	ex vivo	53	59	117	570	GBM
Bury et al. 2020 [77]	ex vivo	96	–	–	1881	meningioma, glioma
Ember et al. 2024 [79]	in vivo	67		668	1329	metastasis, GBM, meningioma
Klamminger et al. 2024 [80]	ex vivo	82	82	–	679	metastasis, GBM, glioma, meningioma
Uckermann et al. 2024 [81]	in vivo	29			218	metastasis, GBM, glioma, meningioma
	ex vivo	48		73	375	
Qingbo Li, Shufan Chen 2024 [82]	–	242	205	265	411	glioma

Study	Mean age	Sample state	Cross validation	Classification algorithm	RS	Ratings of the quality of the evidence (see text for explanation)
Koljenovic et al. 2005 [27]	59	frozen	yes	LDA	NIRS	1
Leslie et al. 2012 [33]	–	fresh, frozen	yes	SVMA	CRM	2
Aguiar et al. 2013 [34]	–	frozen	no	DBA	NIRS	1
Kalkanis et al. 2014 [35]	63.9(GBM), 31.8 (normal)	frozen	no	DFA	CRM	1
Jermyn et al. 2015 [37]	53	fresh	yes	BTC	NIRS	1
Ji et al. 2015 [36]	–	fresh	no	–	SRSM	1
Galli et al. 2019 [38]	–	fresh	yes	QDA	CRM	1
Riva et al. 2021 [29]	–	fresh	yes	–	NIRS	1
Livermore et al. 2021 [40]	–	fresh	yes	LDA	CRM	1
Jabarkheel et al. 2022 [41]	–	fresh	yes	LR	CRM	1
Kopec et al. 2021 [73]	–	fresh	yes	PLS-DA	CRM	1
Auner et al. 2012 [75]	–	fresh and frozen	yes	DFA	CRM	2
Klamminger et al. 2021 [76]	60.34	frozen	yes	SVM	–	–
Bury et al. 2020 [77]	–	frozen	–	LDA, QDA	CRM	–
Ember et al. 2024 [79]	63.5	fresh	no	–	–	–
Klamminger et al. 2024 [80]	–	frozen	yes	RFC	–	1
Uckermann et al. 2024 [81]	–	fresh	–	–	HT	–
	–	–	–	DMS-DLFF	miniature RS	–
Qingbo Li, Shufan Chen 2024 [82]	–	fresh	yes	BTC	HT	–

*tissues, not patients. N1 number of total patients, N2 number of patients in test group (not training), N3 number of tissues, N4 number of spectra. GBM glioblastoma multiforme, NIRS near infrared Raman spectrometer, CRM confocal Raman microscope, SRSM Stimulated Raman scattering microscopy, DRS Dispersive Raman spectrometer, LR Logistic Regression, DBA Distance-based analysis, QDA quadratic discriminant analysis, LDA linear discriminant analysis, SVMA support vector machine analysis, DFA discriminant function analysis, PLSA-DA Partial Least Squares Discriminant Analysis, DFA discriminant function analysis, BTC boosted trees classification, RFC random forest classification, SVM support vector machines, DMS-DLFF deep learning features fusion, HT handheld probe RS "-" means no data was provided by authors.

2.6. Quality assessment

Methodological quality for each study was assessed according to the QUADAS-2 guidelines [32]. All QUADAS-2 items were used to evaluate the eligible articles. Online Appendix 2 presents QUADAS-2 detailed analysis, including bias assessment. Ratings of the quality of the evidence were based on the rating scheme listed below (modified from the Oxford Centre for Evidence-based Medicine for ratings of individual studies [47]): rating 1 – properly powered and conducted randomized clinical trial; systematic review with *meta*-analysis; rating 2 – well-designed controlled trial without randomization; prospective comparative cohort trial; rating 3 – case-control studies; retrospective cohort study; rating 4 – case series with or without intervention; cross-sectional study; rating 5 – opinion of respected authorities; case reports. The results are presented in Table 1.

Detailed information on materials and methodology adopted in each research findings is presented in Appendix 1.

2.7. Statistical analysis

In this *meta*-analysis we calculated pooled sensitivity and specificity, with 95 % confidence intervals (CI), summary receiver operator characteristics (SROC) [44] curves and diagnostic odds ratio (DOR) for every diagnostic test.

As a first step, TP, TN, FP and FN values (spectra count) were extracted from each study and put into Excel sheet. Then all the records were grouped by study ID (last author's name and publication year) and brain tumor type. In this way we received four groups, within which statistical analysis of effectiveness of RS as a diagnostic test was performed: GBM only, all gliomas (including GBM), meningiomas and metastases.

The pooled sensitivity and specificity were calculated based on the DerSimonian Laird method (random effects model). Sensitivity and specificity are pooled by

$$Sen = \frac{\sum_{i=0}^{18} TPi}{\sum_{i=0}^{18} (TPi+FNi)} \text{ and } Spe = \frac{\sum_{i=0}^{18} TNi}{\sum_{i=0}^{18} (TNi+FPi)} \text{ formulas.}$$

SROC curves were constructed to visualize the relationship between sensitivity and specificity. DOR computation method was Moses' constant of linear model.

Potential heterogeneity was explored with *meta*-regression analysis and subgroup analysis. Weighted least squares (inverse variance) was selected as a model estimation method.

Meta Disc version 1.4 was used to perform the above analysis.

3. Results

3.1. Search results

By searching the database, 6112 records were found; after reviews, case studies, conference abstracts were removed, 363 articles remained. 154 duplicates were removed. Of these, the suitability of 64 full-text articles was evaluated. Finally, 18 studies

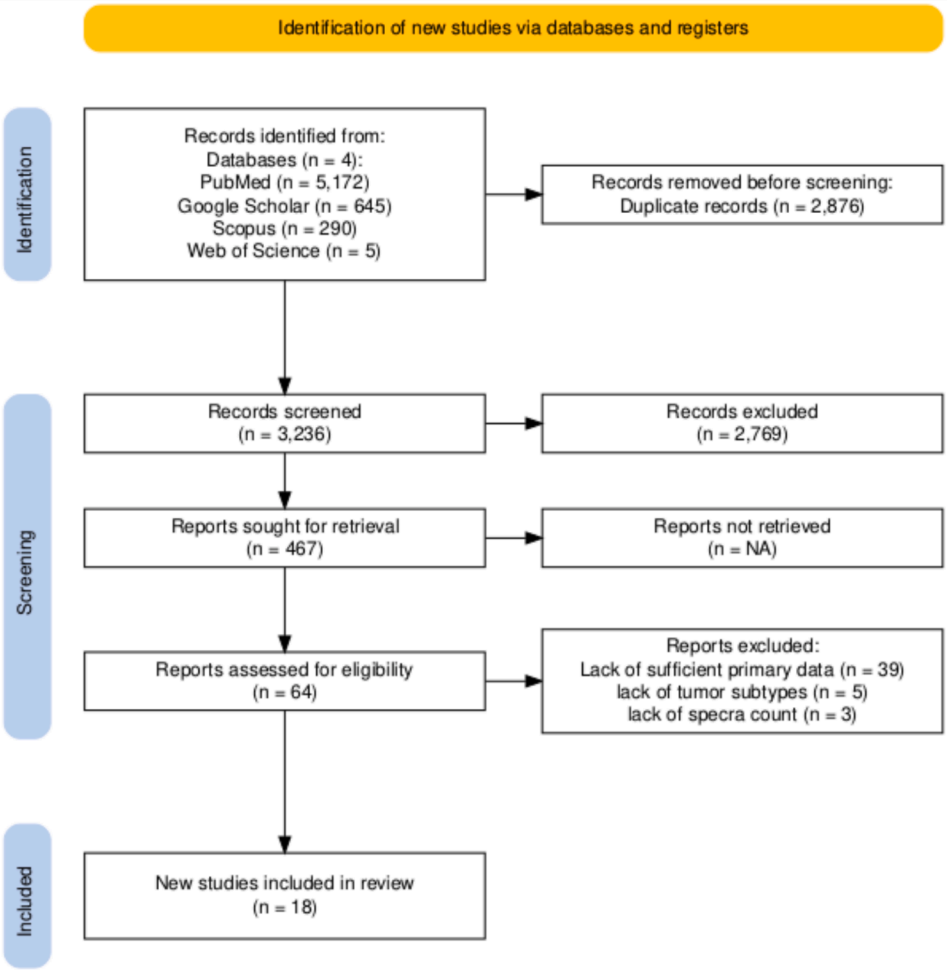

Fig. 1. Flow chart showing search strategy. FromHaddaway, N. R., Page, M. J., Pritchard, C. C., & McGuinness, L. A. (2022). PRISMA2020: An R package and Shiny app for producing PRISMA 2020-compliant flow diagrams, with interactivity for optimised digital transparency and Open Synthesis Campbell Systematic Reviews, 18, e1230. https://doi.org/10.1002/cl2.1230.

[27,29,33–38,40,41,73,75–77,79–82] were reviewed and included into the *meta*-analysis. Fig. 1 shows the study identification process.

The detailed characteristics of the studies are shown in Table 1.

The number of the included patients, if provided, varied from 8 to 242. The number of the spectra retrieved, if provided, varied from 115 to 135600. The total number of spectra was 162299, with an average of 8542 and mean value 678.

Three studies ([37,79,81]) performed RS in vivo during tumor resection surgeries, all other studies based on ex vivo samples.

Six studies [27,34,35,76,77,80] used frozen tissue samples for analysis, ten studies [29,36–38,40,41,73,79,81,82] used fresh tissue samples, while two studies [33,75] used both.

Meningioma was a subject of investigation in seven studies [27,34,38,73,77,79,81], GBM in nine studies [34,35,38,40,73,76,79–81], gliomas in general in thirteen studies [29,33,36–38,40,41,73,75,77,80–82] and metastases in five studies [38,73,79–81].

3.2. Diagnostic accuracy in glioma group

Thirteen studies [29,33,36–38,40,41,73,75,77,80–82] examined glioma. The detailed data for each study is presented in Table 2.

The pooled sensitivity and specificity of RS for discriminating glioma and normal brain tissues were 0,965 (95 % CI 0,962–0,967) and 0,738 (95 % CI 0,736–0,739). Fig. 2 (A and B) demonstrates the forest plots. The pooled DOR was 61,305 (95 % CI 22,758–165,14), which demonstrates that tests are discriminating correctly with high accuracy [45]. The SROC curve analysis was used to summarize overall diagnostic accuracy (Fig. 3 (A)).

3.3. Diagnostic accuracy in GBM group

Nine studies [34,35,38,40,73,76,79–81] examined GBM. The pooled sensitivity and specificity of RS for discriminating GBM and normal brain tissues were 0,948 (95 % CI 0,943–0,952) and 0,506 (95 % CI 0,503–0,509). Fig. 2 (C and D) demonstrates the forest plots. The pooled DOR was 78,420 (95 % CI 29,150–210,97), which demonstrates that tests are discriminating correctly with high accuracy [45]. The SROC curve is shown in Fig. 3 (B).

3.4. Diagnostic accuracy in meningioma group

Seven studies [27,34,38,73,77,79,81] examined meningioma. The pooled sensitivity and specificity of RS for discriminating meningioma and normal brain tissues were 0,896 (95 % CI 0,898–0,894) and 0,913 (95 % CI 0,910–0,916). Fig. 2 (E and F) demonstrates the forest plots. The pooled DOR was 149,59 (95 % CI 23,342–958,68). The SROC curve is shown in Fig. 3 (C).

3.5. Diagnostic accuracy in metastasis group

Five studies [38,73,79–81] examined metastasis. The pooled sensitivity and specificity of RS for discriminating metastasis and normal brain tissues were 0,946 (95 % CI 0,941–0,951) and 0,862 (95 % CI 0,864–0,860). Fig. 2 (G and H) demonstrates the forest plots. The pooled DOR was 133,90 (95 % CI 23,340–768,17). The SROC curve is shown in Fig. 3 (D).

3.6. Between-study heterogeneity

The chi-squared test for homogeneity (likelihood ratio test for sensitivities and specificities and Cochran's Q test based upon inverse

Table 2
Sensitivity, specificity and DOR values for individual studies, calculated based on TP, TN, FP, FN. Grouped by tumor type.

Study	Tumor type	Sample type	Sensitivity,95 % CI	Specificity,95 % CI	DOR,95 % CI
Aguiar et al. 2013	GBM	frozen	0,800 (0,563–0,943)	1,000 (0,962–1,000)	693,00 (35,618–13483,3)
Ember et al. 2024	GBM	fresh	0,909 (0,882–0,932)	0,910 (0,888–0,929)	101,40 (69,227–148,52)
Galli et al. 2019	GBM	fresh	0,945 (0,866–0,985)	1,000 (0,590–1,000)	231,67 (11,336–4734,3)
Kalkanis et al. 2014	GBM	frozen	0,968 (0,955–0,978)	0,997 (0,992–0,999)	9424,2 (3315,3–26789,4)
Klamminger et al. 2021	GBM	frozen	0,806 (0,757–0,849)	0,649 (0,589–0,706)	7,698 (5,264–11,257)
Klamminger et al. 2024	GBM	frozen	0,300 (0,119–0,543)	0,976 (0,915–0,997)	17,143 (3,138–93,657)
Kopec et al. 2021	GBM	fresh	0,950 (0,944–0,955)	0,497 (0,494–0,500)	18,773 (16,768–21,018)
Livermore et al. 2021	GBM	fresh	0,972 (0,964–0,979)	0,718 (0,674–0,759)	88,068 (63,101–122,91)
Uckermann et al. 2024	GBM	fresh	0,800 (0,593–0,932)	0,800 (0,519–0,957)	16,000 (3,229–79,273)
Bury et al. 2020	Glioma	frozen	0,866 (0,843–0,886)	0,352 (0,319–0,385)	3,489 (2,780–4,380)
Galli et al. 2019	Glioma	fresh	0,897 (0,819–0,949)	1,000 (0,768–1,000)	241,67 (13,418–4352,6)
Jabarkheel et al. 2022	Glioma	fresh	0,913 (0,865–0,949)	0,813 (0,755–0,862)	45,713 (25,031–83,482)
Jermyn et al. 2015	Glioma	fresh	0,643 (0,351–0,872)	0,857 (0,421–0,996)	10,800 (0,997–117,00)
Ji et al. 2015	Glioma	fresh	0,940 (0,835–0,987)	1,000 (0,863–1,000)	692,14 (34,391–13930,0)
Klamminger et al. 2024	Glioma	frozen	0,694 (0,563–0,804)	0,796 (0,720–0,859)	8,819 (4,482–17,350)
Kopec et al. 2021	Glioma	fresh	0,979 (0,977–0,982)	0,739 (0,737–0,740)	135,02 (120,83–150,88)
Leslie et al. 2012	Glioma	fresh and frozen	1,000 (0,971–1,000)	0,941 (0,894–0,971)	3873,6 (224,83–66737,0)
Livermore et al. 2021	Glioma	fresh	0,970 (0,963–0,977)	0,683 (0,645–0,719)	0,360 (52,848–93,676)
Qingbo Li, Shufan Chen 2024	Glioma	–	0,965 (0,935–0,984)	0,808 (0,736–0,867)	117,33 (53,863–255,56)
Riva et al. 2021	Glioma	fresh	0,919 (0,906–0,930)	0,696 (0,671–0,721)	26,015 (21,403–31,621)
Uckermann et al. 2024	Glioma	fresh	0,735 (0,556–0,871)	0,808 (0,606–0,934)	11,667 (3,384–40,220)
Auner et al. 2012	Glioma	fresh and frozen	0,938 (0,892–0,969)	0,986 (0,958–0,997)	1037,4 (284,76–3779,5)
Aguiar et al. 2013	Meningioma	frozen	0,897 (0,758–0,971)	1,000 (0,962–1,000)	1491,0 (78,264–28404,9)
Bury et al. 2020	Meningioma	frozen	0,336 (0,300–0,374)	0,895 (0,876–0,911)	4,304 (3,373–5,491)
Ember et al. 2024	Meningioma	fresh	0,949 (0,926–0,967)	0,960 (0,945–0,972)	453,21 (265,43–773,85)
Galli et al. 2019	Meningioma	fresh	1,000 (0,933–1,000)	1,000 (0,590–1,000)	1605,0 (29,581–87082,9)
Koljenovic et al. 2005	Meningioma	frozen	1,000 (0,805–1,000)	1,000 (0,292–1,000)	245,00 (4,124–14555,8)
Kopec et al. 2021	Meningioma	fresh	0,900 (0,902–0,898)	0,912 (0,910–0,915)	93,722 (89,946–97,656)
Uckermann et al. 2024	Meningioma	fresh	not enough data	not enough data	not enough data
Ember et al. 2024	Metastasis	fresh	0,981 (0,959–0,993)	0,960 (0,946–0,971)	1216,8 (511,68–2893,5)
Galli et al. 2019	Metastasis	fresh	1,000 (0,852–1,000)	1,000 (0,590–1,000)	705,00 (12,846–38692,2)
Klamminger et al. 2024	Metastasis	frozen	0,525 (0,361–0,685)	0,855 (0,742–0,931)	6,509 (2,541–16,670)
Kopec et al. 2021	Metastasis	fresh	0,947 (0,942–0,952)	0,861 (0,863–0,859)	110,73 (100,51–121,99)
Uckermann et al. 2024	Metastasis	fresh	0,839 (0,663–0,945)	1,000 (0,832–1,000)	197,55 (10,320–3781,5)

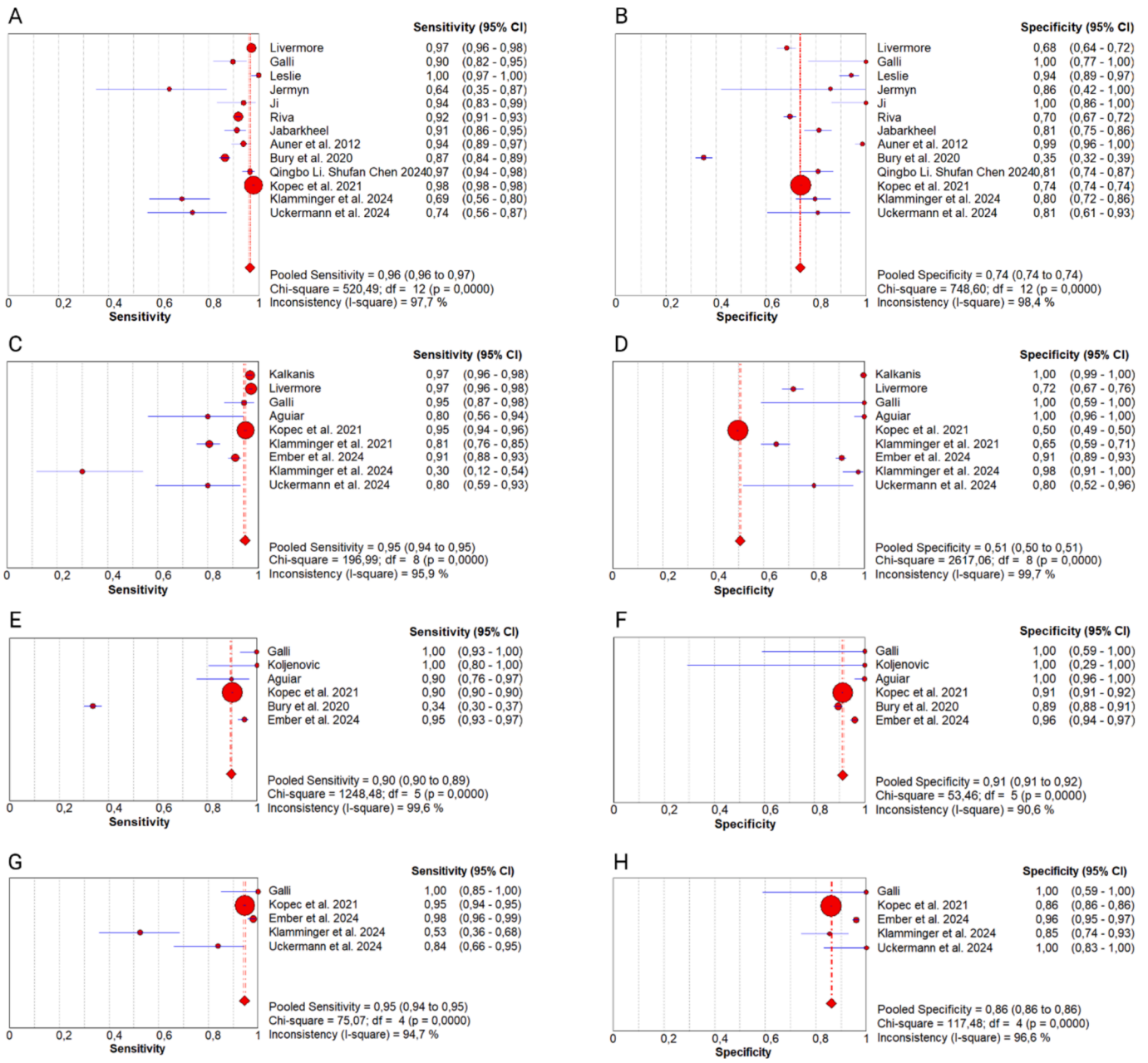

Fig. 2. Individual and pooled values of sensitivity and specificity and their 95% CIs of RS to differentiate normal tissues from glioma (A and B), GBM (C and D), meningioma (E and F) and metastasis (G and H).

variance weights for likelihood ratios and diagnostic odds ratios) and the I-square index were performed. Primarily between-study heterogeneity was substantial or considerable in most outcomes. Potential heterogeneity in sensitivity and specificity was analyzed with *meta*-regression analysis and subgroup analysis. Brain tumor type, sample type (fresh/frozen) and sample acquisition type (ex vivo/in vivo) were used as co-variants in *meta*-regression. None of them could explain the heterogeneity ($p > 0.05$) (see Table 3). Classification algorithm and RS type were not analyzed as not all studies reported these data.

Subgroup analysis by sample type revealed that for fresh sample type pooled sensitivity and specificity were 0,970 and 0,739 for glioma, 0,952 and 0,500 for GBM, 0,900 and 0,913 for meningioma, 0,948 and 0,862 for metastasis.

For frozen sample type pooled sensitivity and specificity were 0,856 and 0,417 for glioma, 0,919 and 0,940 for GBM, 0,382 and 0,902 for meningioma.

4. Discussion

RS is a technique of substance structure identification based on analysis of light scattering off the surface of the substance after it has been illuminated with a laser. The scattered light can provide a lot of information about the structure of the substance and thus can be very helpful in identification and quantification of chemical components. When light is scattered off a surface, it can either have the same energy (and thus the same wavelength and frequency) as the emitted light or a different energy. When the scattered and emitted light have the same energy, this is called Rayleigh or elastic scattering. Raman or inelastic scattering occurs when energy of scattered light is different (frequency shift); this happens when molecule, illuminated with light, absorbs some of that light to excite a molecular vibration. Since the frequencies (wavelength) of light absorbed by a molecule being illuminated are unique to the molecule and type of bonds, detecting these frequencies of

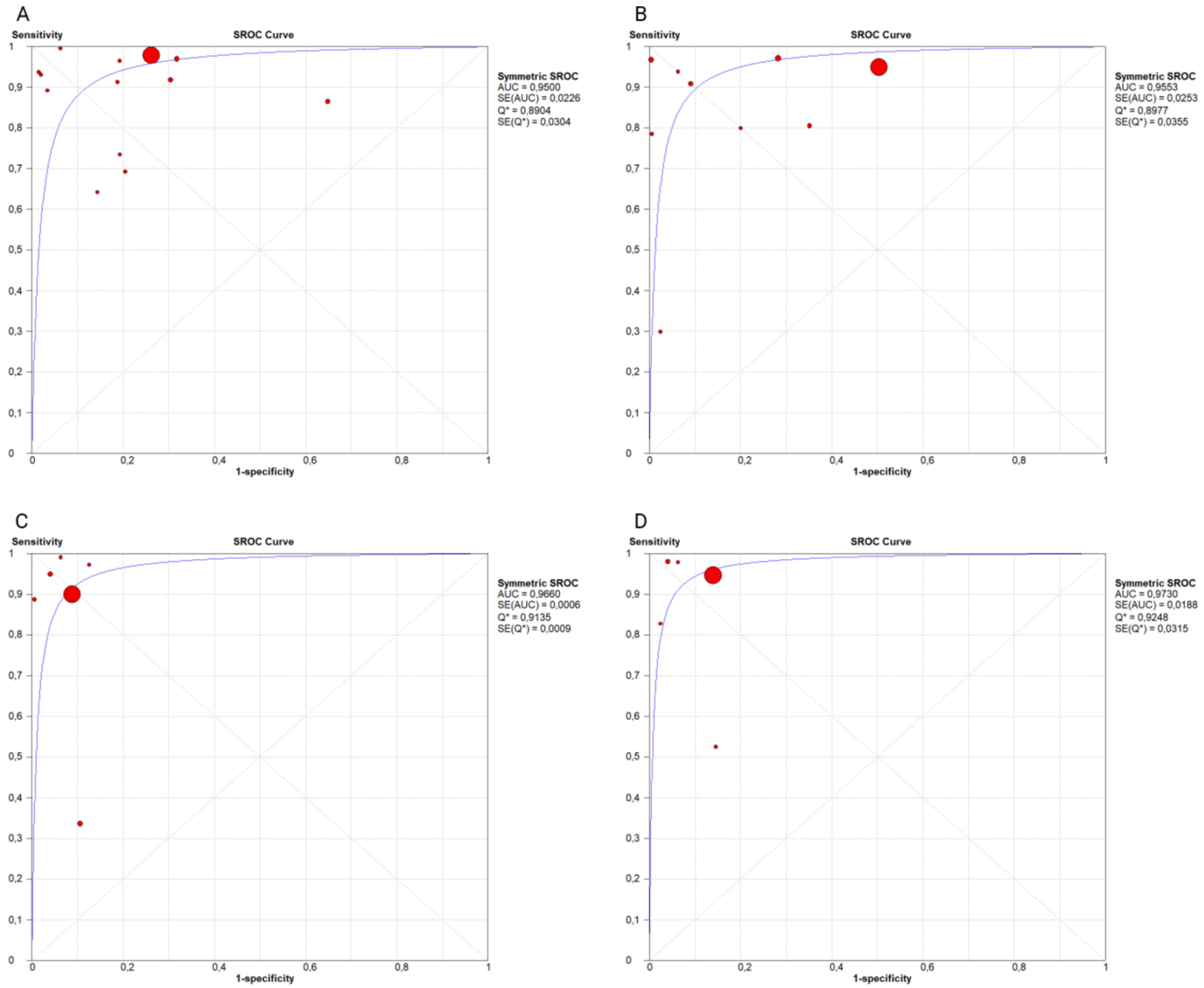

Fig. 3. Summary receiver operating characteristics (SROC) curve of RS to differentiate normal tissues from glioma (A), GBM (B), meningioma (C) and metastasis (D).

Table 3
Relative diagnostic odds ratio (RDOR) of co-variants in the *meta*-regression analysis.

Variant	p-value	RDOR	95 % CI
Sample type	0,7384	1,30	(0,26; 6,40)
Brain tumor type	0,5488	1,27	(0,57; 2,84)
Sample acquisition type	0,9911	1,01	(0,12; 8,89)

light could allow to identify which molecules are present in the substance [16]. The Raman spectrum, which is a plot of Raman shifts, creates so called chemical fingerprint providing information on structure of big range of substances by determining biochemical differences within a biological tissue. Every organic particle has a characteristic vibration frequency which is visualized in the Raman spectrum as a peak. Numerous studies [17–29,43] report assignment of Raman peaks with their biological interpretation. Raman spectra are often recorded in the fingerprint region (400–1800 cm^{-1}) [83]. In this way RS can provide information on the vibrational structure of a tissue and identify main biomolecular alterations at the tissue and cellular level. The most important biomolecular changes which can be detected by RS in brain tumor tissue are: 1) alterations in lipid composition (tumor tissue can have altered lipid metabolism and decreased lipid content, changes in phospho-/sphingolipids or cholesterol bands can be detected by RS) [87]; 2) nucleic acids alterations which is especially helpful in case of some brain tumors with the overexpression of certain genes and a change in DNA or RNA content [86,87]; 3) protein changes (RS can detect elevated protein content, specific for some tumors, or changes in protein structure such as α-helices, β-sheets) [86,87]; 4) metabolic shifts (elevated tyrosine, phenylalanine, and tryptophan levels or increased glycolysis can be associated with tumors) [86,87]; 5) changes in glycosaminoglycans and proteoglycans; 6) changes in vascularization of brain tumor based on presence hemoglobin [87]; 7) identification of tumor-specific biomarkers such as accumulation of lipofuscin or collagen degradation.

To excite a Raman spectrum, there must be a strong source of electromagnetic radiation. The excitation radiation in most of cases is in the form of visible light, but ultraviolet and near-infrared radiation is also used [83]. Using laser waves in the visible light range can cause excitation of fluorescence, which can interfere with the Raman signal and in some cases even cause sample decomposition [83]. This is one of the limitations of RS.

The Raman spectrometer consists of a light source, a monochromator, a sample holder, and a detector [83]. Lasers, used as

excitation light sources in RS, may differ depending on the analyzed tissue type. The choice of wavelength for laser excitation is one of the most important parameters in RS. RS requires no special tissue preparation such as freezing or staining. 2 mm^3 sample size is enough. Therefore no special reagents are required.

The first study on appliance of RS in brain tissue analysis was published in 1990 by Tashibu [84]. At a time, water content in brain tissue was analyzed with RS. Since then, there have been many studies examining the use of RS to analyze the structure of brain tumors and distinguish them from healthy brain tissue [50,85,63,67–70]. As a step further, researchers have investigated the possibilities of RS appliance in differentiation of brain tumor types (primary vs metastatic) and subtypes of primary brain tumors along with molecular markers (low-grade gliomas vs high-grade, brain tumors subtypes according to WHO classification) [39,59,71,72]. Moreover, several studies have reported appliance of RS for differentiation of necrotic, infiltrative and vital regions of brain tumor [18,60]. The ability to distinguish healthy brain tissue from regions of tumor infiltration is crucial for gross total resection and thus the patient's prognosis.

Most of available studies applying RS on brain tissues perform Raman analysis ex vivo – tissue sample is excised, washed in 0,9% saline solution and put onto a spectrometer slide for further analysis. In order to enable repeatable measurements, the same acquisition parameters must be applied such as temperature, number of sampling points, exposure time, number of spectral accumulations, power of the laser etc. Afterwards, the data needs to be preprocessed (i.e. noise subtraction, vector normalization) in a certain repeatable way, before the statistical analysis could be conducted. To sum up, in case of ex vivo RS, the cost estimate should include, apart from the spectrometer itself and the station for data processing with appropriate software, the costs of daily technical maintenance and calibration of the spectrometer so that all the measurements are performed in accordance with the developed protocol.

Jermyn et al [37], Herta et al [42], Uckermann et al [81] and Qingbo Li, Shufan Chen [82] proved that RS could be successfully applied in vivo, using handheld probe without making harm to a patient. For example Jermyn et al [37] developed a handheld contact fiber optic RS probe capable of single-point submillimeter Raman signal detection. The probe, containing fiber optic cables which were connected to a NIR spectrum–stabilized lase, was connected to a high-speed and high-resolution charge-coupled device spectroscopic detector. The laser and the imaging spectrometer were sending Raman spectra to a computer in real time (see Fig. 4).

Desroches et al [61] have developed and presented first in-human use of a RS guidance system integrated with a brain biopsy needle.

In this *meta*-analysis we have succeeded do identify eighteen studies investigating appliance of RS in differentiation of brain tumor tissue from healthy one with distinguishing of a tumor type [27,29,33–38,40,41,73,75–77,79–82] which are built in a way allowing to calculate pooled sensitivity and specificity of the method. More than 162,000 spectra were included in the *meta*-analysis. RS was proved to distinguish healthy brain tissue from glioma with 96,5% pooled sensitivity, 73,8% pooled specificity, from GBM with 94,8% pooled sensitivity, 50,6% pooled specificity, from meningioma with 89,6% pooled sensitivity, 91,3% pooled specificity and from metastasis with 94,6% pooled sensitivity, 86,2% pooled specificity. The pooled DORs for glioma, GBM, meningioma and metastasis were 61,3, 78,4, 149,6 and 133,9 respectively.

The DOR is a measure of test performance combining the strengths of sensitivity and specificity, as prevalence independent indicators, it can be used even as a single indicator. It ranges from zero to infinity; the higher the DOR, the better test performance is. When DOR is less than one, the test is in the wrong direction, while a DOR of exactly one means that the test the test gives no information [64].

Ji et al [36] differed from other included studies, as its object of study was accuracy of Stimulated Raman scattering (SRS) microscopy. SRS uses two synchronized pulse lasers, a pump beam and a Stokes beam, to coherently excite the vibration of molecules. When the frequency difference between the Stokes and pump beams equals the vibration frequency of a chemical bond, the intensity of pump beam decreases and the intensity of the Stokes beam increases, which is detected by SRS microscopy [46]. SRS microscopy could be widely used for imaging biomolecules in cells such as lipids, cholesterol, proteins, nucleic acids. It has been also used for direct imaging of different types of tissues and organs such as brain or skin [46]. SRS microscopy presents results with a speed, specificity and resolution [46]. Illustrative comparison of SRS and traditional microscopy of intrinsic brain tumors can be found in Ji et al [36].

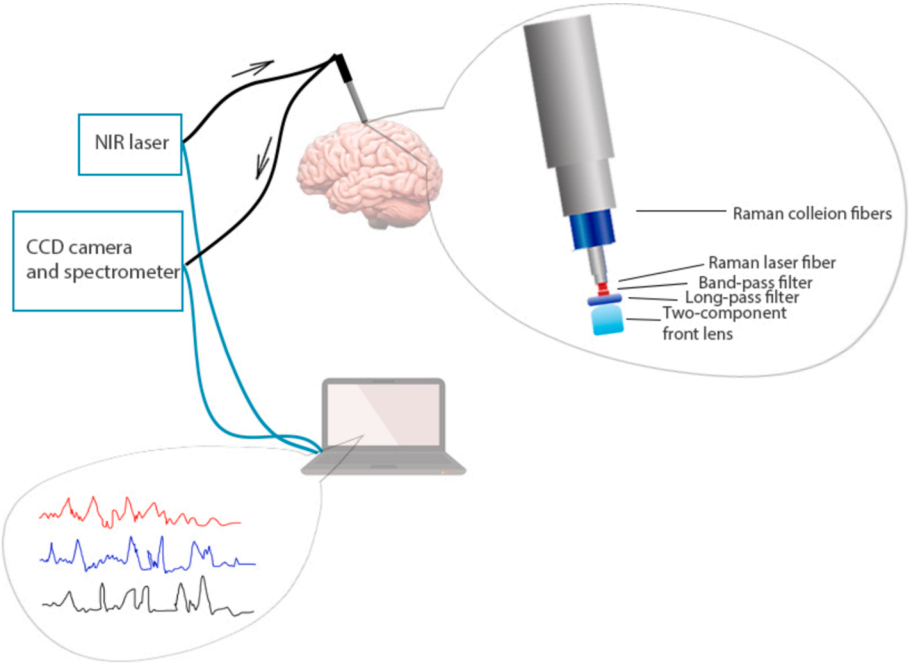

Fig. 4. The handheld probe for Raman spectroscopy – drawn based on Herta et al [42].

Although Herta et al [42] was excluded from the *meta*-analysis due to lack of data for reconstruction of 2x2 table, authors of the manuscript felt strong need to mention the study as it compared in vivo RS with 5-ALA and showed that RS was capable to detect tumor-infiltrated brain with higher sensitivity but lower specificity than 5-ALA.

This *meta*-analysis aimed to assess the accuracy of RS in differentiation of normal brain tissue from brain tumor. The *meta*-analysis proved that RS has a potential of being successfully used for accurate brain tumor identification intraoperatively – primarily for tumor borders identification, enabling total tumor resection, and secondarily during brain tumor biopsy aiming to avoid reoperation in cases of non-diagnostic first biopsy. In both cases spectral analysis could be performed right after sample is retrieved in a traditional way, within several minutes after sample retrieval, or in vivo on live tissue.

The *meta*-analysis has its limitations. Primarily between-study heterogeneity was substantial or considerable in most outcomes which weakens the robustness of the results. Potential sources of bias are: number of spectra analyzed per each study; different techniques of RS and different classification algorithms; different sample states: fresh/frozen, ex vivo/in vivo; possible contamination of samples with blood; repeatable conditions and settings of RS may not have been maintained within each study.

We see certain limitations of RS itself for brain tumor tissue rapid identification. Although RS doesn't require reagents or tissue preparation (apart from sample washing with saline solution), a spectroscope should be used by a qualified person and further spectral analysis should be performed by an expert in the area. In order to enable intraoperative appliance of RS for brain tumor identification and differentiation, there is a need for automatic neural classifiers. Apart from that, repeatable conditions for RS should be guaranteed in order to assure reliable results.

5. Conclusions

Raman spectroscopy has a potential to serve as a tool for differentiation of brain tumors from normal brain tissue. Not only could it be helpful in distinguishing a malignant lesion from benign with high sensitivity and specificity, but also indicate the type of tumor.

RS was proved to distinguish healthy brain tissue from glioma with 0,965 sensitivity and 0,738 specificity, from GBM in particular with 0,948 sensitivity and 0,506 specificity, from meningioma with 0,896 sensitivity and 0,913 specificity, from metastasis with 0,946 sensitivity and 0,862 specificity. The DOR within particular brain tumor groups was high: 61,305 for gliomas, 78,420 for GBM, 149,59 for meningioma and 133,90 for metastasis, which indicates RS is an effective performance test.

Due to the small count of patients in a majority of available studies, more clinical trials with essential amount of patients are required to further evaluate the accuracy of RS. More reports on RS appliances in vivo using hand-held probe are required. More studies investigating accuracy of RS in differentiation of brain tumor subtypes are required, especially studies on classification of genetic subtypes of high-grade and low-grade gliomas by detecting specific gene mutations such as Isocitrate dehydrogenase 1 mutation.

Author contributions

All authors contributed to the study conception and design. Data collection and preparation were performed by AK. Statistical analyses were performed by AK. The first draft of the manuscript was written by AK. Writing reviewing and editing was performed by MK-G and BC. All authors read and approved the final manuscript.

8. Data Sharing Statement

The datasets generated during and/or analyzed during the current study are available from the corresponding author on reasonable request.

Ethical approval and consent to participate

Not applicable.

10. Human and animal ethics

Not applicable.

11. Consent for publication

Not applicable.

Funding

The authors declare that no grants, funds or other support were received during the writing of this manuscript.

Declaration of competing interest

The authors declare that they have no known competing financial interests or personal relationships that could have appeared to influence the work reported in this paper.

Appendix A. Supplementary data

Supplementary data to this article can be found online at https://doi.org/10.1016/j.saa.2024.125518.

Data availability

Data will be made available on request.

References

[1] San Diego Brain Tumor foundation. Facts and statistics on brain tumors. https://www.sdbtf.org/resources/brain-tumor-facts/. Accessed February 03, 2024.
[2] American Brain Tumor Association. Brain tumor education. https://www.abta.org/about-brain-tumors/brain-tumor-education/. Accessed February 03, 2024.
[3] End Brain Cancer. Brain Tumor Statistics. https://endbraincancer.org/brain-tumor-statistics/. Accessed February 12, 2024.
[4] Aaron Cohen-Gadol. 72 Must-Know Brain Tumor Statistics. https://www.aaroncohen-gadol.com/en/patients/brain-tumor/types/statistics. Accessed March 23, 2024.
[5] Onyije FM, Dolatkhah R, Olsson A et al. Risk factors for childhood brain tumours: A systematic review and meta-analysis of observational studies from 1976 to 2022. Cancer Epidemiol. 2024; 88:102510. [PubMed] [PMC free article].
[6] L.M. Wang, Z.K. Englander, M.L. Miller, B.JN. Malignant, Glioma, Adv Exp Med Biol. 1405 (2023) 1–30 [PubMed].
[7] P. Śledzińska, M.G. Bebyn, J. Furtak, J. Kowalewski, M.A. Lewandowska, Prognostic and predictive biomarkers in gliomas, Int J Mol Sci. 22 (19) (2021) 10373 [PMC free article].
[8] A.C. Tan, D.M. Ashley, G.Y. López, M. Malinzak, H.S. Friedman, M. Khasraw, Management of glioblastoma: State of the art and future directions, CA Cancer J Clin. 70 (2020) 299–312, https://doi.org/10.3322/caac.21613 [PubMed] [CrossRef] [Google Scholar].
[9] P.C.D.W. Hamer, M. Klein, S.L. Hervey-Jumper, J.S. Wefel, M.S. Berger, Functional outcomes and health-related quality of life following glioma surgery, Neurosurgery. 88 (4) (2021) 720–732 [PMC free article].
[10] R. Sun, H. Cuthbert, C. Watts, Fluorescence-guided surgery in the surgical treatment of gliomas: past present and future, Cancers (basel) 13 (14) (2021) 3508 [PMC free article].
[11] Kumar GK, Balasubramaniam A, Pradeep K, Manohar N. Intraoperative MRI in Brain Tumor Surgeries [published online March 28, 2021]. Frontiers in Clinical Neurosurgery. doi: 10.5772/intechopen.95588.
[12] S. Cui, S. Zhang, S. Yue, Raman Spectroscopy and Imaging for Cancer Diagnosis, J Healthc Eng. 8619342 (2018), https://doi.org/10.1155/2018/8619342. PMID: 29977484; PMCID: PMC6011081.
[13] M. Jermyn, J. Desroches, K. Aubertin, et al., A review of Raman spectroscopy advances with an emphasis on clinical translation challenges in oncology, Phys Med Biol. 61 (23) (2016) R370–R400, https://doi.org/10.1088/0031-9155/61/23/R370. PMID: 27804917.

[14] M. Brusatori, G. Auner, T. Noh, L. Scarpace, B. Broadbent, S.N. Kalkanis, Intraoperative raman spectroscopy, Neurosurg Clin N Am. 28 (4) (2017) 633–652, https://doi.org/10.1016/j.nec.2017.05.014. PMID: 28917291.
[15] Bruker. Raman Basics. Guide to Raman Spectroscopy. https://www.bruker.com/en/products-and-solutions/infrared-and-raman/raman-spectrometers/what-is-raman-spectroscopy.html. Accessed April 01, 2024.
[16] C.V. Raman, K.S. Krishnan, A new type of secondary radiation, Nature. 121 (3048) (1928) 501–502, https://doi.org/10.1038/121501c0.
[17] L.J. Livermore, M. Isabelle, I.M. Bell, et al., Raman spectroscopy to differentiate between fresh tissue samples of glioma and normal brain: A comparison with 5-ALA–induced fluorescence-guided surgery, J Neurosurg. 1–11 (2020) [CrossRef].
[18] É. Lemoine, F. Dallaire, R. Yadav, et al., Feature engineering applied to intraoperative: In vivo Raman spectroscopy sheds light on molecular processes in brain cancer: A retrospective study of 65 patients, Analyst. 144 (2019) 6517–6532 [CrossRef].
[19] C. Krafft, S.B. Sobottka, G. Schackert, R. Salzer, Raman and infrared spectroscopic mapping of human primary intracranial tumors: A comparative study, J. Raman Spectrosc. 37 (2006) 367–375 [CrossRef].
[20] J. Zhao, H. Lui, D.I. McLean, H. Zeng, Automated autofluorescence background subtraction algorithm for biomedical Raman spectroscopy, Appl Spectrosc. 61 (2007) 1225–1232 [CrossRef].
[21] N. Bergner, C. Krafft, K.D. Geiger, M. Kirsch, G. Schackert, J. Popp, Unsupervised unmixing of Raman microspectroscopic images for morphochemical analysis of non-dried brain tumor specimens, Proc Anal Bioanal Chem. 403 (2012) 719–725 [CrossRef].
[22] Z. Movasaghi, S. Rehman, I.U. Rehman, Raman spectroscopy of biological tissues, Appl Spectrosc Rev. 42 (2007) 493–541 [CrossRef].
[23] M. Brusatori, G. Auner, T. Noh, L. Scarpace, B. Broadbent, S.N. Kalkanis, Intraoperative raman spectroscopy, Neurosurg Clin N Am. 28 (2017) 633–652 [PubMed].
[24] O. Aydin, M. Altas, M. Kahraman, O.F. Bayrak, M. Culha, Healthy brain tissue and tumors using surfaceenhanced Raman scattering, Appl Spectrosc. 63 (2009) 1095–1100 [PubMed].
[25] M. Köhler, S. MacHill, R. Salzer, Ch. Krafft, Characterization of lipid extracts from brain tissue and tumors using Raman spectroscopy and mass spectrometry, Anal Bioanal Chem. 393 (2009) [CrossRef].
[26] R.E. Kast, G.W. Auner, M.L. Rosenblum, et al., Raman molecular imaging of brain frozen tissue sections, J Neurooncol. 120 (2014) 55–62 [PubMed].
[27] S. Koljenovic, T.B. Schut, A. Vincent, J.M. Kros, G.J. Puppels, Detection of meningioma in dura mater by Raman spectroscopy, Anal Chem. 77 (2005) 7958–7965 [CrossRef].
[28] A. Beljebbar, S. Dukic, N. Amharref, et al., Ex vivo and in vivo diagnosis of C6 glioblastoma development by Raman spectroscopy coupled to a microprobe, Anal Bioanal Chem 398 (477–487) (2010) [CrossRef].
[29] M. Riva, T. Sciortino, R. Secoli, M. Manfait, Glioma biopsies classification using raman spectroscopy and machine learning models on fresh tissue samples, Cancers. 13 (2021) 1073, https://doi.org/10.3390/cancers13051073.
[30] M.J. Page, J.E. McKenzie, B.PM. The, Prisma,, et al., statement: an updated guideline for reporting systematic reviews [published online March 29, 2021], BMJ. 372 (2020) n71, https://doi.org/10.1136/bmj.n71.
[31] PRISMA Statement. Preferred Reporting Items for Systematic Reviews and Meta-Analyses. http://www.prisma-statement.org/. Accessed March 03, 2024.
[32] QUADAS. Quality assessment of studies. https://www.bristol.ac.uk/population-health-sciences/projects/quadas/quadas-2/. Accessed March 11, 2024.
[33] D.G. Leslie, R.E. Kast, J.M. Poulik, et al., Identification of Pediatric Brain Neoplasms Using Raman Spectroscopy, Pediatr Neurosurg. 48 (2012) 109–117, https://doi.org/10.1159/000343285.
[34] R.P. Aguiar, L. Silveira, E.T. Falcao, M.T.T. Pacheco, R.A. Zângaro, C. A. Pasqualucci, Discriminating neoplastic and normal brain tissues in vitro through raman spectroscopy: a principal components analysis classification model, Photomedicine and Laser Surgery. 31 (2013) 595–604, https://doi.org/10.1089/pho.2012.3460.
[35] S.N. Kalkanis, R.E. Kast, M.L. Rosenblum, et al., Raman spectroscopy to distinguish grey matter, necrosis, and glioblastoma multiforme in frozen tissue sections, J Neurooncol. 116 (2014) 477–485, https://doi.org/10.1007/s11060-013-1326-9.
[36] M. Ji, S. Lewis, S. Camelo-Piragua, et al., Detection of human brain tumor infiltration with quantitative stimulated Raman scattering microscopy, Science Translational Medicine. 7 (309) (2015) 163, https://doi.org/10.1126/scitranslmed.aab0195.
[37] M. Jermyn, K. Mok, J. Mercier, et al., Intraoperative brain cancer detection with Raman spectroscopy in humans, Science Translational Medicine. 7 (274) (2015) 19, https://doi.org/10.1126/scitranslmed.aaa2384.
[38] R. Galli, M. Meinhardt, E. Koch, et al., Rapid Label-Free Analysis of Brain Tumor Biopsies by Near Infrared Raman and Fluorescence Spectroscopy—A Study of 209 Patients, Front Oncol. 9 (2019) 1165, https://doi.org/10.3389/fonc.2019.01165.
[39] L.J. Livermore M. Isabelle I.M. Bell et al. Rapid intraoperative molecular genetic classification of gliomas using Raman spectroscopy Neuro-Oncology Advances. XX (XX) 1–12 2019 10.1093/noajnl/vdz008.
[40] L.J. Livermore, M. Isabelle, I.M. Bell, et al., Raman spectroscopy to differentiate between fresh tissue samples of glioma and normal brain: a comparison with 5-ALA-induced fluorescence-guided surgery, J Neurosurg. 135 (2020) 469–479, https://doi.org/10.3171/2020.5.JNS20376.
[41] R. Jabarkheel, C.S. Ho, A.J. Rodrigues, et al., Rapid intraoperative diagnosis of pediatric brain tumors using Raman spectroscopy: a machine learning approach, Neuro-Oncology Advances. 4 (2022) 1–7, https://doi.org/10.1093/noajnl/vdac118.
[42] J. Herta, A. Cho, T. Roetzer-Pejrimovsky, et al., Optimizing maximum resection of glioblastoma: Raman spectroscopy versus 5-aminolevulinic acid, J Neurosurg. 139 (2023) 334–343, https://doi.org/10.3171/2022.11.JNS22693.
[43] Banerjee HN, Zhang L. Deciphering the finger Prints of Brain Cancer Astrocytoma in comparison to Astrocytes by using near infrared Raman Spectroscopy. Mol Cell Biochem. 2007;295, 237–240. [CrossRef].
[44] F. Li, H. He, Assessing the Accuracy of Diagnostic Tests, Shanghai Arch Psychiatry. 30 (3) (2018) 207–212, https://doi.org/10.11919/j.issn.1002-0829.218052. [PMC free article].
[45] Šimundić AM. Measures of Diagnostic Accuracy: Basic Definitions. EJIFCC 2009;19 (4):203-11. [PMC free article].
[46] L. Shi, A.A. Fung, A. Zhou, Advances in stimulated Raman scattering imaging for tissues and animals, Quant Imaging Med Surg. 11 (3) (2021) 1078–1101, https://doi.org/10.21037/qims-20-712 [PMC free article].
[47] Howick J, Chalmers I, Glasziou P et al. Explanation of the 2011 Oxford Centre for Evidence-Based Medicine (OCEBM) Levels of Evidence (Background Document). Oxford Centre for Evidence-Based Medicine. https://www.cebm.ox.ac.uk/resources/levels-of-evidence/ocebm-levels-of-evidence. Accessed April 28, 2024.
[48] J. Desroches, M. Jermyn, K. Mok, et al., Characterization of a Raman spectroscopy probe system for intraoperative brain tissue classification. Biomedical Optic, Express. 6 (7) (2015), https://doi.org/10.1364/BOE.6.002380.
[49] B. Kideog, W. Zheng, K. Lin, et al., Epi-detected Hyperspectral Stimulated Raman Scattering Microscopy for Label-free Molecular Subtyping of Glioblastomas, Anal. Chem. (2018), https://doi.org/10.1021/acs.analchem.8b01677.
[50] H. Abramczyk, A. Imiela, B. Brozek-Pluska, M. Kopec, Advances in Raman imaging combined with AFM and fluorescence microscopy are beneficial for oncology and cancer research, Nanomedicine (lond.) 14 (14) (2019) 1873–1888, https://doi.org/10.2217/nnm-2018-0335.
[51] R. Galli, O. Uckermann, A. Temme, et al., Assessing the efficacy of coherent anti-Stokes Raman scattering microscopy for the detection of infiltrating glioblastoma in fresh brain samples, J Biophotonics. 10 (3) (2017 Mar) 404–414, https://doi.org/10.1002/jbio.201500323.
[52] N. Neidert, J. Straehle, D. Erny, et al., Stimulated Raman histology in the neurosurgical workflow of a major European neurosurgical center - part A, Neurosurg Rev. 45 (2) (2022 Apr) 1731–1739, https://doi.org/10.1007/s10143-021-01712-0.
[53] C. Krafft, B. Belay, N. Bergner, et al., Advances in optical biopsy – correlation of malignancy and cell density of primary brain tumors using Raman microspectroscopic imaging, Analyst 137 (2012) 5533–5537, https://doi.org/10.1039/C2AN36083G.
[54] O. Uckermann, W. Yao, T.A. Juratli, et al., IDH1 mutation in human glioma induces chemical alterations that are amenable to optical Raman spectroscopy, J Neurooncol. 139 (2) (2018) 261–268, https://doi.org/10.1007/s11060-018-2883-8.
[55] F. Dallaire, F. Picot, J.P. Tremblay, et al., Quantitative spectral quality assessment technique validated using intraoperative in vivo Raman spectroscopy measurements, J Biomed Opt. 25 (4) (2020) 1–8, https://doi.org/10.1117/1.
[56] I. Romanishkin, T. Savelieva, A. Kosyrkova, et al., Differentiation of glioblastoma tissues using spontaneous Raman scattering with dimensionality reduction and data classification, Front Oncol. 15 (12) (2022) 944210, https://doi.org/10.3389/fonc.2022.944210.
[57] F.K. Lu, D. Calligaris, O.I. Olubiyi, et al., Label-Free Neurosurgical Pathology with Stimulated Raman Imaging, Cancer Res. 76 (12) (2016) 3451–3462, https://doi.org/10.1158/0008-5472.
[58] N. Bergner, B.F. Romeike, R. Reichart, et al., Tumor margin identification and prediction of the primary tumor from brain metastases using FTIR imaging and support vector machines, Analyst. 138 (14) (2013) 3983–3990, https://doi.org/10.1039/c3an00326d.
[59] T.C. Hollon, S. Lewis, B. Pandian, et al., Rapid intraoperative diagnosis of pediatric brain tumors using stimulated raman histology, Cancer Res. 78 (1) (2018) 278–289, https://doi.org/10.1158/0008-5472.
[60] K. Klein, G.G. Klamminger, L. Mombaerts, et al., Computational Assessment of Spectral Heterogeneity within Fresh Glioblastoma Tissue Using Raman Spectroscopy and Machine Learning Algorithms, Molecules. 29 (5) (2024 Feb 23) 979, https://doi.org/10.3390/molecules29050979.
[61] J. Desroches, É. Lemoine, M. Pinto, et al., Development and first in-human use of a Raman spectroscopy guidance system integrated with a brain biopsy needle, J Biophotonics. 12 (3) (2019 Mar) e201800396.
[62] C.L.M. Morais, T. Lilo, K.M. Ashton, et al., Determination of meningioma brain tumour grades using Raman microspectroscopy imaging, Analyst. 144 (23) (2019 Nov 18) 7024–7031, https://doi.org/10.1039/c9an01551e.
[63] D. Reinecke, N. von Spreckelsen, C. Mawrin, et al., Novel rapid intraoperative qualitative tumor detection by a residual convolutional neural network using label-free stimulated Raman scattering microscopy, Acta Neuropathol Commun. 10 (1) (2022 Aug 6) 109, https://doi.org/10.1186/s40478-022-01411-x.
[64] A. Glas, J. Lijmer, M. Prins, et al., The diagnostic odds ratio: a single indicator of test performance, Journal of Clinical Epidemiology 56 (11) (2003) 1129–1135, https://doi.org/10.1016/S0895-4356(03)00177-X. ISSN 0895-4356,.
[65] J. Desroches, M. Jermyn, M. Pinto, et al., A new method using Raman spectroscopy for in vivo targeted brain cancer tissue biopsy, Scientific Reports 8 (2018) 1792, https://doi.org/10.1038/s41598-018-20233-3 2.
[66] A. Ospanov, I. Romanishkin, T. Savelieva, et al., Optical differentiation of brain tumors based on raman spectroscopy and cluster analysis methods, Int J Mol Sci. 24 (19) (2023) 14432, https://doi.org/10.3390/ijms241914432.
[67] A.A. Kowalska, S. Berus, Ł. Szleszkowski, et al., Brain tumour homogenates analysed by surface-enhanced Raman spectroscopy: Discrimination among healthy

and cancer cells, Spectrochim Acta A Mol Biomol Spectrosc. 15 (231) (2020) 117769, https://doi.org/10.1016/j.saa.2019.117769.
[68] E. Baria, F. Giordano, R. Guerrini, et al., Dysplasia and tumor discrimination in brain tissues by combined fluorescence, Raman, and diffuse reflectance spectroscopies, Biomed Opt Express. 14 (3) (2023) 1256–1275, https://doi.org/10.1364/BOE.477035.
[69] R.P. Aguiar, E.T. Falcão, C.A. Pasqualucci, L. Silveira Jr., Use of Raman spectroscopy to evaluate the biochemical composition of normal and tumoral human brain tissues for diagnosis, Lasers Med Sci. 37 (1) (2022 Feb) 121–133, https://doi.org/10.1007/s10103-020-03173-1.
[70] J. Liu, P. Wang, H. Zhang, N. Wu, Distinguishing brain tumors by Label-free confocal micro-Raman spectroscopy, Photodiagnosis Photodyn Ther. 45 (2024) 104010, https://doi.org/10.1016/j.pdpdt.2024.104010.
[71] A. Imiela, B. Polis, L. Polis, H. Abramczyk, Novel strategies of Raman imaging for brain tumor research, Oncotarget. 8 (49) (2017) 85290–85310, https://doi.org/10.18632/oncotarget.19668.
[72] B. Polis, A. Imiela, L. Polis, H. Abramczyk, Raman spectroscopy for medulloblastoma, Childs Nerv Syst. 34 (12) (2018) 2425–2430, https://doi.org/10.1007/s00381-018-3906-7.
[73] M. Kopec, M. Błaszczyk, M. Radek, H. Abramczyk, Raman imaging and statistical methods for analysis various type of human brain tumors and breast cancers, Spectrochim Acta A Mol Biomol Spectrosc. 262 (2021) 120091, https://doi.org/10.1016/j.saa.2021.120091.
[74] M. Jermyn, J. Mercier, K. Aubertin, et al., Highly accurate detection of cancer in situ with intraoperative, label-free, Multimodal Optical Spectroscopy. Cancer Res. 77 (14) (2017) 3942–3950, https://doi.org/10.1158/0008-5472.CAN-17-0668.
[75] A.W. Auner, R.E. Kast, R. Rabah, J.M. Poulik, M.D. Klein, Conclusions and data analysis: a 6-year study of Raman spectroscopy of solid tumors at a major pediatric institute, Pediatr Surg Int. 29 (2) (2013) 129–140, https://doi.org/10.1007/s00383-012-3211-6.
[76] G.G. Klamminger, J.J. Gérardy, F. Jelke, et al., Application of Raman spectroscopy for detection of histologically distinct areas in formalin-fixed paraffin-embedded glioblastoma, Neurooncol Adv. 3 (1) (2021) vdab077, https://doi.org/10.1093/noajnl/vdab077.
[77] D. Bury, C.L.M. Morais, F.L. Martin, et al., Discrimination of fresh frozen non-tumour and tumour brain tissue using spectrochemical analyses and a classification model, Br J Neurosurg. 34 (1) (2020) 40–45, https://doi.org/10.1080/02688697.2019.1679352.
[78] D. Bury, C.L.M. Morais, K.M. Ashton, T.P. Dawson, F.L. Martin, Ex vivo raman spectrochemical analysis using a handheld probe demonstrates high predictive capability of brain tumour status, Biosensors (basel). 9 (2) (2019) 49, https://doi.org/10.3390/bios9020049.
[79] K. Ember, F. Dallaire, A. Plante, et al., In situ brain tumor detection using a Raman spectroscopy system-results of a multicenter study, Sci Rep. 14 (1) (2024) 13309, https://doi.org/10.1038/s41598-024-62543-9.
[80] G.G. Klamminger, L. Mombaerts, F. Kemp, et al., Machine learning-assisted classification of paraffin-embedded brain tumors with raman spectroscopy, Brain Sciences. 14 (4) (2024) 301, https://doi.org/10.3390/brainsci14040301.
[81] O. Uckermann, J. Ziegler, M. Meinhardt, et al., Raman and autofluorescence spectroscopy for in situ identification of neoplastic tissue during surgical treatment of brain tumors, J Neurooncol. (2024), https://doi.org/10.1007/s11060-024-04809-w.
[82] Q. Li, S. Chen, Glioma identification based on digital multimodal spectra integrated with deep learning feature fusion using a miniature raman spectrometer, Appl Spectrosc. 37028241276013 (2024), https://doi.org/10.1177/00037028241276013.
[83] A. Saletnik, B. Saletnik, C. Puchalski, Overview of popular techniques of raman spectroscopy and their potential in the study of plant tissues, Molecules. 26 (6) (2021) 1537, https://doi.org/10.3390/molecules26061537.
[84] K. Tashibu, Analysis of water content in rat brain using Raman spectroscopy, No to Shinkei. 42 (1990) 999–1004.
[85] I. Romanishkin, T. Savelieva, A. Kosyrkova, Differentiation of glioblastoma tissues using spontaneous Raman scattering with dimensionality reduction and data classification, Front. Oncol. 12 (2022) 944210, https://doi.org/10.3389/fonc.2022.944210.
[86] S. Elsheikh, N.P. Coles, O.J. Achadu, P.S. Filippou, A.A. Khundakar, Advancing brain research through surface-enhanced raman spectroscopy (SERS): current applications and future prospects, Biosensors. 14 (1) (2024) 33, https://doi.org/10.3390/bios14010033.
[87] J.C. Ranasinghe, Z. Wang, S. Huang, Raman Spectroscopy on Brain Disorders: Transition from Fundamental Research to Clinical Applications, Biosensors (basel). 13 (1) (2022) 27, https://doi.org/10.3390/bios13010027. PMID: 36671862; PMCID: PMC9855372.